Optik - International Journal for Light and Electron Optics 212 (2020) 164673

Contents lists available at ScienceDirect

Optik

journal homepage: www.elsevier.com/locate/ijleo

Original research article

# Design of frame-type support structure for space-based rectangular convex mirror tested on the back

Wang Kejun[a,*], Dong Jihong[a], Wang Xiaoyu[a], Chi Chunyan[b]

[a] Changchun Institute of Optics, Fine Mechanics and Physics, Chinese Academy of Sciences, Changchun 130033, China
[b] Jilin Jianzhu University, Changchun 130118, China

ARTICLE INFO

*Keywords:*
Space remote sensor
The frame-type support structure
The simulation analysis
Surface shape error test
Mechanical test

ABSTRACT

In view of the functional requirements of high reliability support and high stability support of rectangular convex mirror of space remote sensor, at the same time, considering the development cost and lead time, a frame-type support structure for rectangular mirror tested on the back of space remote sensor was designed, which included a support frame and two groups of flexible grooves. In-depth study was done about support principle and engineering realization of the space-based mirror support. The error sources of surface shape errors of space-based mirror assembly were summarized. Two groups of flexible structures were designed and their positions were reasonably arranged, so as to effectively eliminate or alleviate the surface shape errors caused by various error sources. The statics and dynamics simulation were carried out in view of the design result with the means of finite element analysis, then the test was carried out on the actual mirror subassembly. Experimental results show the surface shape error of mirror with the frame-type support structure is better than$\lambda/60(\lambda = 632.8nm)$, the displacement of mirror is smaller than 0.008mm,the inclination angle is smaller than 1.5″. The mirror assembly has a reasonable distribution of modal, the fundamental frequency is 256 Hz, which is higher than the requirement of 120 Hz. Under the sin and random vibration, the acceleration amplification were 1.1 and 4.2 times respectively, and the dynamic stress under two test conditions were 14.5MPa and 128MPa respectively, The simulation and test results show that the support effect of the frame-type support structure is good, meets the high reliability and high stability support demand of rectangular convex mirror of space remote sensor.

## 1. Introduction

Space remote sensor are used for the survey and detailed investigation of earth and space resources, and have important scientific and economic significance in the field of earth observation and space exploration. The optical component of space remote sensor – mirror subassembly is the most important component in the whole optical system. Under the influence of gravity load, temperature load, assembly error and other factors, the mirror surface often deforms seriously. [1–3]

The supporting forms of mirrors are mainly divided into three categories [4–6]: passive supporting forms, gravity unloading forms and active optical forms. Passive support is a traditional support method. The larger the diameter of the mirror, the more complex the structure of passive support and the more difficult the design. However, its reliability is high and its performance is stable. Active optics is a new support technology, which can adjust the size of the driving force in real time to correct the mirror surface shape error

* Corresponding author.
*E-mail address:* wangkejun1@163.com (W. Kejun).

https://doi.org/10.1016/j.ijleo.2020.164673
Received 16 February 2020; Accepted 30 March 2020

and ensure the imaging quality of the system. Gravity unloading can be said to be a semi-active optical form. On the ground, a certain number of gravity unloading devices are applied to the mirror to simulate the on-orbit environment, so that its surface shape error can meet the requirements of the index. During the on-orbit operation, gravity disappears, the gravity unloading device is disconnected, and the mirror surface shape error remains unchanged.

For passive support, the back three-point support is a very effective form of support, and the back three-point support structure is suitable for mirrors with a diameter of less than 2000 mm for space applications (for mirrors with a smaller diameter, such as under 200 mm, the center single-point support is more appropriate) with good results. However, the back three-point support structure cannot be used to support the rectangular convex mirror using the back offner detection scheme. For rectangular convex mirror, the use of the classical Hindle method to use the large diameter auxiliary spherical mirror for the test of no difference point inevitably has the defect of center blocking, and often because of the auxiliary spherical mirror diameter is too large, resulting in difficult processing and adjustment, and the lead time is very long [7].

For the effective support of the rectangular convex mirror which was tested with the back offner test scheme, a new frame-type support structure with double flexible groove was proposed, which is suitable for rectangular convex mirror with back offner test scheme. The influence to the mirror surface shape error due to gravity load, temperature load and assembly error was greatly weakened with this kind of support structure, and the mirror subassembly had a good modal distribution and dynamic stiffness which met the requirements [8].

## 2. Principle of mirror support

To realize the stable support of the mirror, two points should be guaranteed: to realize the spatial positioning of the mirror and to ensure the relative position relationship between each mirror. Ensure the precision of mirror surface shape. For the first point, the mirror is treated as a rigid body and the 6 degrees of freedom of mirror should be constrained. For the second point, the mirror is treated as an elastomer to reduce its deformation.

To realize spatial positioning, the six spatial degrees of freedom of the mirror should be constrained according to the mechanism kinematics principle. The support form should be statically indeterminate support or super-statically indeterminate support.

Means to reduce the deformation of the mirror body and ensure the precision of the mirror surface shape: to improve the structure stiffness of the mirror itself, such as using lightweight structure to improve the equivalent structure stiffness or using high-stiffness materials. Increase the number of support points, for the same stiffness of the mirror body, the bending deformation of the mirror body will be smaller [9,10].

## 3. Rectangular convex mirror model and related parameters

In order to realize the back offner detection scheme of rectangular convex mirror, fused quartz suitable for lens material was selected. The rectangular convex mirror has a optical aperture of 89 × 74.5 mm and its vertex radius of curvature is 494.39 mm. In order to avoid edge effect during mirror processing, processing allowance was reserved for the mirror body. The geometric size of the mirror body is 99 × 85 mm, and the detailed structure is shown in Fig. 1.

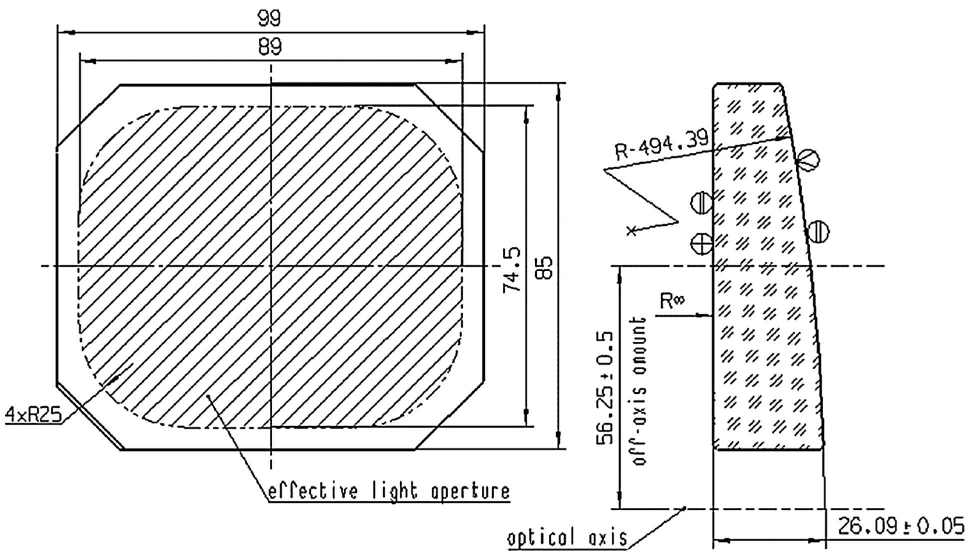


**Fig. 1.** Mirror body structure parameters.

## 4. Design and optimization of support structure

### 4.1. Index analysis

The design indexes of mirror subassembly mainly include mirror surface shape error, rigid body displacement, inclination angle, mass and dynamic performance.

1) The mirror surface shape error of the mirror assembly (RMS) is smaller than$\lambda/60$ ($\lambda = 632.8$ nm) under the influence of a combination of factors.
2) Under the gravity load, the displacement of the mirror in the direction of gravity is smaller than 0.008 mm.
3) Under the gravity load, the inclination angle of the mirror in the direction of gravity is smaller than 1.5″.
4) The first fundamental frequency of the mirror assembly is larger than 120 Hz.
5) The dynamic stress is smaller than 800Mpa which is the allowable stress of the material of flexible structure.
6) The mass of the mirror subassembly is smaller than 0.8 kg.

Surface shape error is something related to the stiffness of the mirror body, the number of supporting points and the reasonable supporting structure.

Rigid body displacement is something related to the stiffness of the supporting structure. The samller the stiffness of the supporting structure is, the larger the rigid body displacement will be.

Inclination Angle is something related to the supporting position of the supporting structure. The supporting points in the support pass through the center of gravity of the mirror, which can decrease the inclination angle of the mirror.

Dynamic performance is something related to the stiffness of each structural member. On the condition that the mirror surface shape error under temperature load and assembly error meet their index component, the stiffness of each component in the mirror subassembly is increased to the utmost to obtain the higher stiffness of the mirror subassembly.

Mass for a space remote sensor is proportional to launch cost, so we should decrease the components mass while the performance of mirror subassembly is good.

Among the above indexes, the displacement of the mirror body, the inclination angle of the mirror body and the dynamic performance of the mirror subassembly have the same requirements for the stiffness of the support structure, the higher the better. In addition, the inclination angle of the mirror body is also related to the position of the support. On the premise of the mirror subassembly's good performance, the lighter the mass of mirror subassembly, the better. The above indexes are relatively easy to obtain. The mirror surface shape error of mirror subassembly is relatively complex, on which there are many error sources that have an impact. The mirror surface shape error is smaller, the design is more difficult. so it is necessary to carry out targeted design for various error sources, which requires to clarify the errors that affect the mirror surface shape error. After the research, it is concluded that the surface shape error of the mirror has four components: the residual mirror surface shape error caused by the processing of the mirror surface, the mirror surface shape error caused by the disappearance of gravity load, the mirror surface shape error caused by temperature load and the surface shape error caused by assembly.

### 4.2. Index allocation

Mirror surface shape error of mirror subassembly is an index of the most critical and most difficult to guarantee, in order to clear the support structure design goal, the index allocation is carried out to quantify mirror surface shape error components caused by the four error sources which total index is 10.55 nm, as long as each actual error component is smaller than the corresponding allocated error component, the actual total surface shape error will be smaller than the total surface shape error index which is 10.55 nm [11].

The causes of these four errors are different and approximately unrelated. Therefore, the error synthesis formula Eqn 1 of random error and systematic error can be used to calculate the total error.

$$\sigma = \sqrt{\sum_{i=1}^{q} \sigma_i^2 + \sum_{j=1}^{s} s_j^2} \tag{1}$$

Where$\sigma_i$ is the random error and Sj is the single undetermined system error.

Given the current optical mirror surface processing ability, mechanical parts processing precision and the mirror subassembly assembly capacity, the total surface shape error of $\lambda/ 60$ (10.55 nm) was decomposed into five components(including some margin), as shown in the Fig. 2, it was helpful to carry out the targeted design.

In order to facilitate the design, in addition to the allocation of the error of the total surface shape, the allocation of displacement under gravity load and component mass of the mirror subassembly should also be carried out. The mass and displacement are also constraints. The displacement of mirror is caused by the deformation of the mirror body and the supporting structure under the gravity load. To ensure that the total displacement is smaller than the design index, the deformation of the mirror body and the supporting structures under the gravity load should be smaller than the corresponding allocated component index respectively. The same is true for mass. The inclination angle of the mirror body under the gravity load is determined by the supporting position. The fundamental frequency is also a constraint of the mirror assembly. While optimizing the the surface shape error index, the fundamental frequency of the mirror subassembly should be higher than the corresponding design index which is 120 Hz, so a compromise

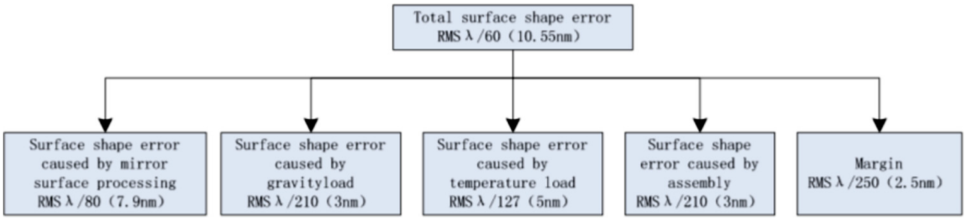


**Fig. 2.** Surface shape error allocation of mirror component.

design needs to be carried out.

### *4.3. Structure design*

Mirror surface shape error testing methods of convex mirror are various, mainly including the Hindle null compensation test method, the back offner test method and the front test method.

The null compensation principle of Hindle test method directly use the focus property of the hyperboloids as the conjugated aberration-free point. The testing light path of convex mirror with Hindle compensator is shown as Fig. 3. The size of Hindle compensator mirror is large which size is about 1 m, which has a long lead time, poor universality and high cost.

The principle of the front test method is to use a flat convex aspheric auxiliary lens with a diameter similar to that of the convex mirror. The testing light path of convex mirror with the flat convex aspheric auxiliary lens for the convex mirror is shown in Fig. 4. The problem is that the processing of flat convex aspheric auxiliary lens needs to use the Offner compensator back test scheme to test its aspheric surface. In other words, the processing of flat convex aspheric auxiliary lens needs to make a set of Offner compensator in advance, which also has the disadvantages of long lead time and high cost.

The offner test method on the back of the convex mirror uses the offner compensator during the test. The compensator is composed of two smaller lenses. The lens is made from transmissive glass, and the back of the convex mirror is processed into a plane surface. The testing light path is shown in Fig. 5. The compensator of this test method is simple in structure, low in cost and short in lead time.

Compared with the other two test methods, the back offner test method is preferred.

By analyzing the supporting principle, error induction and index allocation of the space-based mirror, and considering the characteristics of the rectangular convex mirror, the test method and the system state in installation and adjustment when the optical axis of the mirror is in the horizontal direction, the design constraints and design objectives of the convex mirror subassembly involved in this paper are clarified. It is determined that the rectangular convex mirror adopts the frame-type support structure scheme [12–17].

Mirror subassembly includes mirror, invar part, flexible structure (including flexible groove), support frame (including flexible groove) and adjustment pad.

The mirror material is fused quartz material with good optical transmissibility. The mirror body is solid structure with high absolute stiffness. The detailed supporting structure is shown in Fig. 6.

Adjustment pad is to ensure that the mirror body is in the theoretical position when the mirror subassembly is installed to the main frame.

Invar part is a transition between the mirror and support structure. Support structure to relieve assembly stress, thermal stress on which the flexible groove is included usually choose the titanium alloy material which performance is stable and has a low density. Because the linear expansion coefficient of titanium alloy material is much larger than that of the mirror material, the mirror surface shape error will be worsen because of thermal stress if the support structure with titanium alloy material is directly bonded to the mirror under the temperature load. Therefore, the bonding part which material is invar steel is bonded to the mirror, connecting the

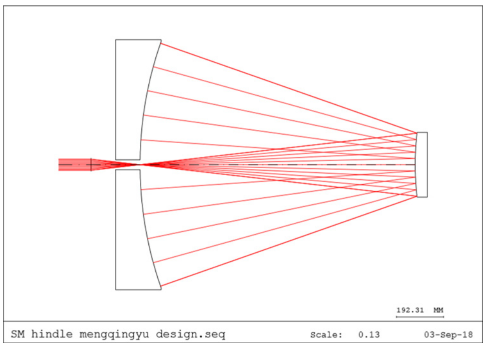


**Fig. 3.** Hindle null compensation test method.

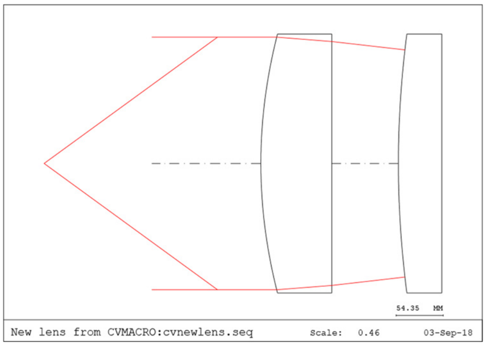


**Fig. 4.** Front test method.

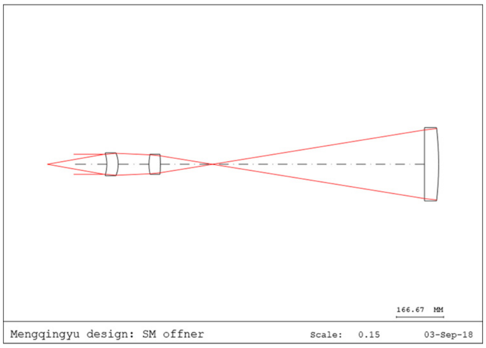


**Fig. 5.** Back offner test method.

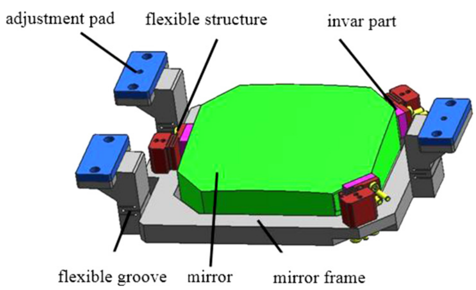


**Fig. 6.** Mirror subassembly.

support structure through the screw holes on the bonding part on the other side. The linear expansion coefficient of invar steel can be adjusted to be consistent with the mirror by adjusting its material ratio, so as to effectively avoid the thermal stress caused by temperature load.

Flexible structure is the connection part between the mirror frame and the mirror in the frame-type support scheme which is the key part of the support structure. The flexible groove is mainly used to relieve the thermal stress between the mirror and the other structure including mirror frame and the external structure because of inconsistent linear expansion coefficient, to relieve the assembly stress at the same time. Three groups of flexible structure are applied simultaneously, distributed in the edge of the mirror. at the same time, in order to avoid deteriorating the mirror surface shape error because of the overturning moment under gravity load, flexible groove center of flexible structure should align to the neutral surface of mirror. The installation position schematic diagram of flexible structure is shown in Fig. 7.

One side of the flexible structure is connected with the invar part, and the other side is connected with the mirror frame. There are three groups of flexible grooves on the flexible structure, which can effectively relieve the thermal stress and partial assembly stress of the mirror assembly. The detailed structure is shown in Fig. 8.

The mirror frame is a frame-type structure with a central light-through hole, which was used to test the mirror surface shape error on the back of the mirror. Flexible grooves are designed on the three supporting legs of the frame, whose main function is to alleviate the assembly stress between the mirror frame and the mounting flange face of the external structure as well as the stress because of the deformation of the external structure, at the same time which can absorb part of the thermal stress. The detailed structure is shown in Fig. 9.

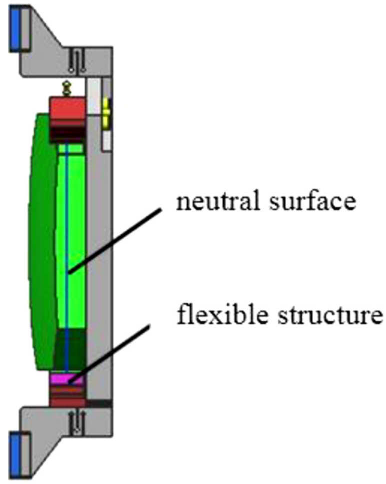


**Fig. 7.** The installation position schematic diagram of flexible structure.

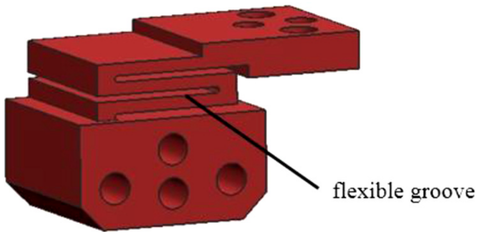


**Fig. 8.** Flexible structure.

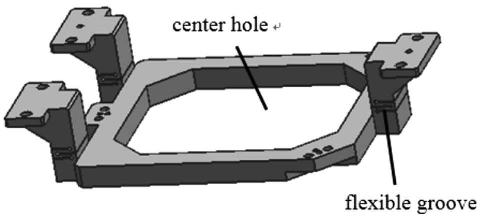


**Fig. 9.** Mirror frame.

The error sources of the mirror surface shape error mainly includes four components. The mirror surface shape error caused by the temperature load and the assembly error is inversely proportional to the flexibility of the support structure, the bigger the flexibility is, the smaller the surface shape error is. But the big flexibility will lead to a lower fundamental frequency and a larger dynamic stress of flexible groove. So we need to have a compromise design, for which a integrated simulation optimization technique is used to carry out the optimization. The integrated optimization platform which is established by the Isight software integrating 3D modeling software, finite element software and matlab software as shown in Fig. 10.

In the optimization process, the minimum of the mirror surface shape error caused by the gravity load, temperature load and

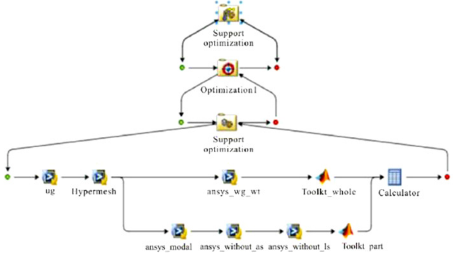


**Fig. 10.** Integrated optimization platform.

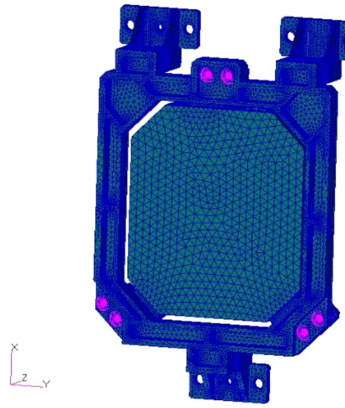

**Fig. 11.** Finite element model of mirror component.

assembly error is defined as the objective function, the mass of the mirror subassembly and the fundamental frequency are defined as constraints, the flexible parameter of support structure including the flexible slice thickness, groove length, groove width and structure size of mirror frame are defined as optimization variables, using optimization algorithm, accomplishing the optimization of flexible and other structural parameters. The support structure of the mirror with the best comprehensive performance is obtained finally.

## 5. Engineering analysis

In the field of engineering, finite element simulation is more and more widely used, mainly for early finding of design defects, optimization and performance evaluation of design schemes. Combined with the requirements of various environmental simulation experiments of the space-based mirror subassembly, the coupling static simulation of force load, temperature load and assembly error and dynamic simulation of the mirror subassembly were carried out in a targeted manner [18–20]. The second order tetrahedral solid element is used to establish the finite element model of the mirror subassembly, as shown in Fig. 11.

### *5.1. The coupling statics analysis of force load, temperature load and assembly error*

In order to verify the statics characteristics of the mirror subassembly, the mirror subassembly was subjected to gravity load which is 1 g, temperature load which is 4℃, and non-flatness error of 0.02 mm on the three supporting points. Under the coupling load, the mirror surface shape error was 3.2 nm. The displacement cloud of mirror subassembly under coupling load was shown in Fig. 12, and the mirror surface shape cloud picture of mirror subassembly is shown in Fig. 13. When 1 g gravity load was applied alone, the mirror surface shape error was 1.1 nm, the mirror displacement in the direction of gravity load was 0.004 mm, and the inclination angle was 0.19 ". When the non-flatness error of 0.02 mm was applied alone, the mirror surface shape error was 1.5 nm, all of which met the requirements of the allocated error component respectively.

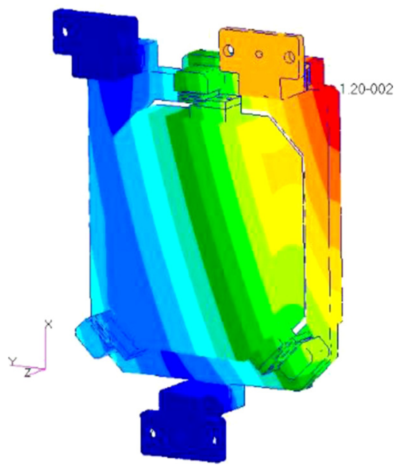


**Fig. 12.** The displacement cloud picture of mirror subassembly with coupling load.

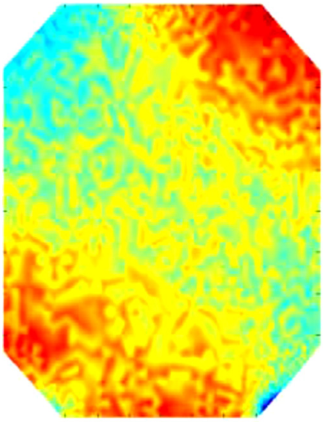

**Fig. 13.** The mirror surface shape cloud picture of mirror subassembly with coupling load.

### *5.2. Dynamic analysis*

Mirror subassembly may be destroyed in the process of transport and emission because of the vibration, impact, overload, so the mirror subassembly should have a high enough stiffness and strength, have a reasonable dynamic stiffness characteristics, have a reasonable dynamic response under the external excitation to ensure that the dynamic stress is smaller than the yield limit of the material. Modal analysis, sine vibration response analysis and random vibration response analysis ware carried out on the mirror subassembly.

Modal analysis showed that the fundamental frequency of the mirror subassembly was 259 Hz, which was much higher than the 120 Hz required by the design, indicating that the structural module had a sufficiently high dynamic stiffness. The natural mode was the oscillation around the Y-axis. The natural mode of vibration is shown in Fig. 14.

In the mechanical vibration test of the remote sensor, a sensor was pasted at the installation of the mirror subassembly, which data obtained can be used as the mechanical vibration condition of the mirror subassembly. The mechanical vibration conditions for the sine vibration response analysis and the random vibration response analysis are shown in Tables 1 and 2. By the sine vibration response analysis and the random vibration response analysis, the response magnification of the mirror subassembly and the dynamic stress at the flexible groove can be obtained.

The response analysis of sine vibration shows that the maximum stress was located in the flexible groove of the flexible structure, the maximum stress in the X direction was 14 MPa, the maximum stress in the Y direction was 13.5 MPa, and the maximum stress in the Z direction was 16 MPa, all of which were located in the flexible groove of the flexible structure. The maximum stress position is shown in Fig. 15, where the vibration stress curve of the most dangerous point in the X direction is shown in Fig. 16. The maximum amplification of acceleration response in X, Y and Z directions was at 100 Hz. The maximum magnification in the X direction was 1.09 times, the maximum magnification in the Y direction was 1.04 times, and the maximum magnification in the Z direction was 1.03 times. The response curve of sine vibration acceleration in the X direction is shown in Fig. 17.

Random vibration response analysis shows that the statistical stress of most dangerous position in the X direction was 93 MPa (3σ), the statistical stress of most dangerous position in the Y direction was 132 MPa (3σ), the statistical stress of most dangerous position in the Z direction was 65 Mpa (3σ), all of which were located in the flexible groove. The stress distribution state of flexible structure under the random vibration in X direction is shown in Fig. 18. The amplification of the total root mean square acceleration in the X direction was 4.34 times. The amplification of the total root mean square acceleration in the Y direction was 3.72 times. The amplification of the total root mean square acceleration in the Z direction was 2.82 times. The response curve of the random vibration

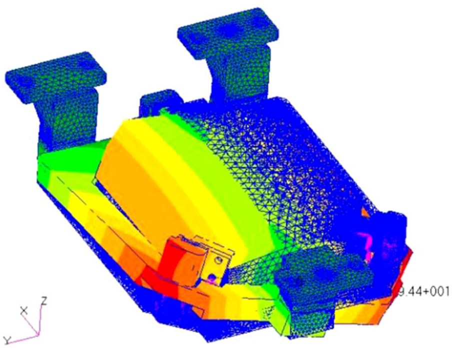


**Fig. 14.** The first natural vibration mode.

**Table 1**
The sine vibration test condition of the mirror assembly.

| Direction | X | | Y | | Z | |
|---|---|---|---|---|---|---|
| Parameters | frequency(Hz) | magnitude | frequency(Hz) | magnitude | frequency(Hz) | magnitude |
| | 5～18 | 6.44 mm(O–P) | 5～20 | 8.08 mm(O–P) | 5～15 | 6.62 mm(O–P) |
| | 18～70 | 8.4g | 20～80 | 13g | 15～60 | 6g |
| | 70～100 | 13g | 80～100 | 8.5g | 60～100 | 12.5g |
| Scan frequency | 2oct/min | | | | | |

**Table 2**
The random vibration test condition of the mirror assembly.

| Direction | X | | Y | | Z | |
|---|---|---|---|---|---|---|
| Parameters | frequency(Hz) | magnitude | frequency(Hz) | magnitude | frequency(Hz) | magnitude |
| | 20～100 | +6dB/oct | 20～100 | +6dB/oct | 20～100 | +6dB/oct |
| | 100～500 | 0.08 g2/Hz | 100～500 | 0.15 g2/Hz | 100～500 | 0.08 g2/Hz |
| | 500～2000 | −12 dB/oct | 500～2000 | −12 dB/oct | 500～2000 | −12 dB/oct |
| | 476～516 0.0001 g2/Hz | | 393～433 0.015g2/Hz | | 230～270 0.0001 g2/Hz | |
| | | | | | 350～436 0.0001 g2/Hz | |
| Total rms acceleration(grms) | 6.68g | | 9.3g | | 6.065g | |
| Testing time(min) | 2 | | | | | |

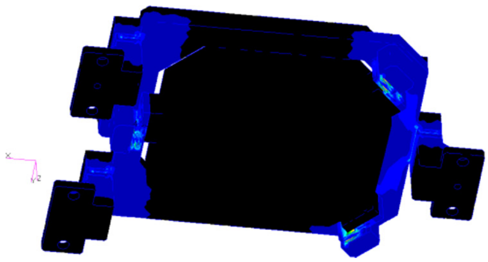

**Fig. 15.** The stress distribution of flexible structure under the sine vibration.

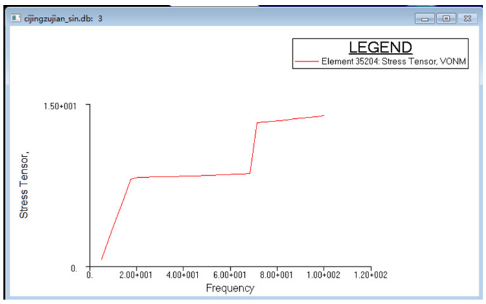


**Fig. 16.** Dynamic stress curve of the most dangerous position of the flexible structure in x direction.

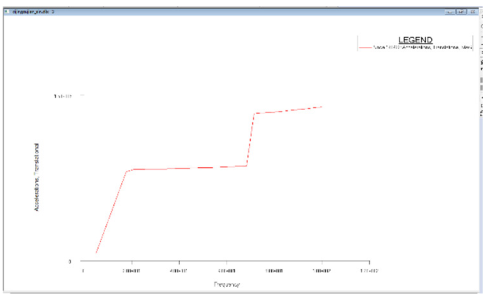


**Fig. 17.** The sine vibration acceleration response curve in x direction.

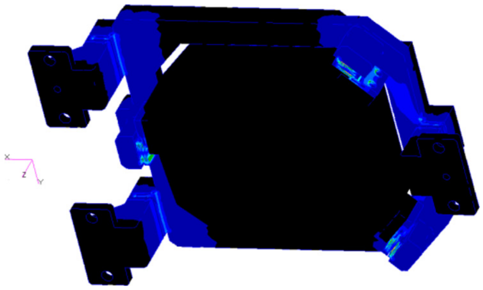

**Fig. 18.** The stress distribution of flexible structure under the random vibration.

acceleration in the X direction was shown in Fig. 19. The random vibration stress response curve in x direction is shown in Fig. 20.

## 6. Experimental verification

When the mirror surface shape error was larger than the 0.1λ(λ = 632.8 nm), the mirror was processed in the form of single mirror. When the mirror surface shape error was about 0.1λ,the invar part was bonded to the mirror and the support structures were integrated with the mirror. Then the mirror was processed in the form of mirror subassembly. The coating of mirror surface will be done when the mirror surface shape error reachedλ/60.Coating will not change the mirror surface shape error and other performance. All environmental experiments should be done before coating. The mirror subassembly is shown in Fig. 21.

### 6.1. Test of mirror surface shape error

The mirror surface shape error was tested by the zygo interferometer which test state was that the optical was horizontal under the coupling load that included gravity load which was 1 g, temperature load which was 24℃ on the basis of room temperature 20℃ and a non-flatness error of 0.02 mm.The mirror surface shape error was 0.0164λat 0°around the optical axis, while 0.0165λwhen the mirror subassembly rotated 180°around the optical axis. After mechanical vibration test, the mirror surface shape error was unvarying. The testing of mirror surface shape error is shown in Fig. 22 and the interferogram of mirror subassembly under coupling load at 0°around the optical axis is shown in Fig. 23.

### 6.2. Test of displacement and inclination angle

The requirements of the displacement and inclination angle of the mirror subassembly were tested by the digital display micrometer and leica theodolite respectively. The test results were obtained after data processing, the displacement of mirror body under gravity load was about 0.006 mm, and the inclination angle was about 1.2″, which of both were better than the design index value.

### 6.3. Mechanical test

The mechanical vibration test was carried out on the mirror subassembly, and the dynamic characteristics of the mirror subassembly were measured, including the dynamic acceleration response magnification of the mirror body and the dynamic stress at the weakest position of the mirror subassembly. The testing site of the mechanical vibration test is shown in the Fig. 24. The sine vibration and random vibration tests in X, Y and Z directions were carried out on the mirror subassembly. The test results showed that the fundamental frequency of the mirror subassembly was 256 Hz, which was basically consistent with the mechanical simulation results. The acceleration response amplification in X, Y and Z directions of sine vibration was 1.1 times, 1.06 times and 1.02 times respectively, and the dynamic stress was 12Mpa, 14Mpa and 14.5Mpa respectively.

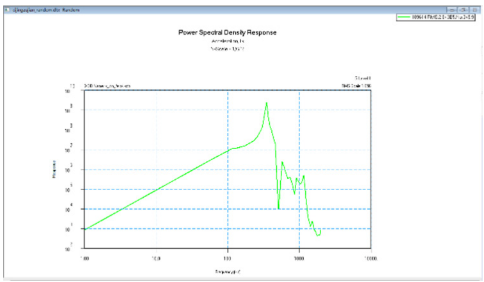


**Fig. 19.** The random vibration acceleration response curve in x direction.

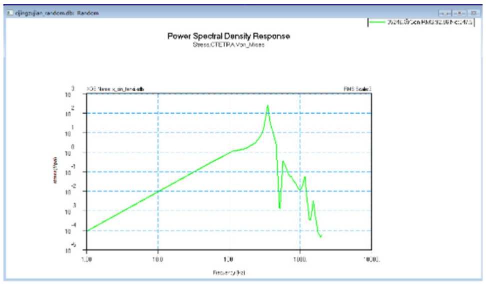


**Fig. 20.** The random vibration stress response curve in x direction.

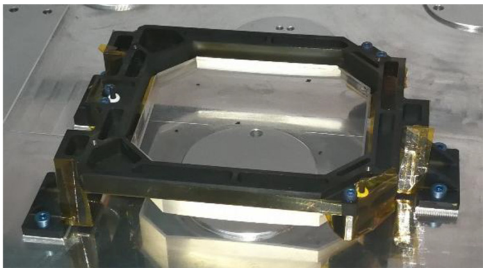

**Fig. 21.** The mirror subassembly.

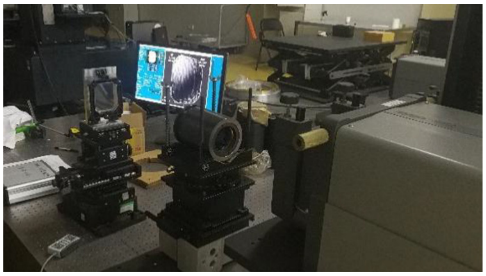

**Fig. 22.** Test of surface shape error.

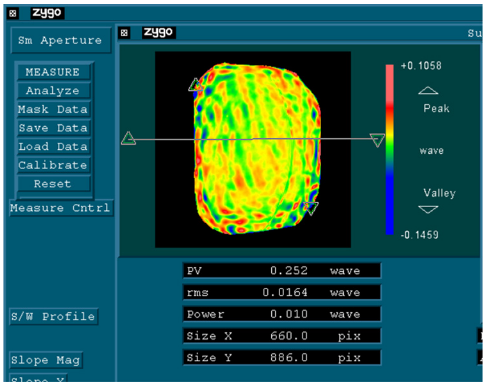


**Fig. 23.** The ZYGO testing interferogram.

The total root-mean-square acceleration magnification in X, Y and Z directions of the random vibration was 4.2 times, 3.65 times and 2.75 times respectively, and the maximum dynamic stress was 89Mpa, 125Mpa and 68Mpa, respectively.

## 7. Conclusion

In order to meet the requirements of high accuracy and stability of the mirror subassembly of the space remote sensor, the supporting principle of the mirror was studied, and the sources of the error causing the mirror surface shape error were analyzed in

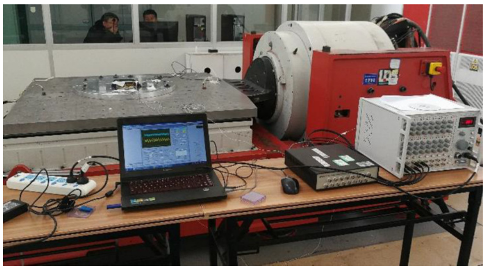

**Fig. 24.** Test of mechanical vibration.

detail. A frame-type flexible support structure to which the back offner test method can be applied and which can adapt to multiple error sources was obtained. The simulation analysis and experimental verification were carried out on the mirror subassembly. The surface shape error of the mirror subassembly under coupling loads was λ/61, better thanλ/60. The mirror displacement is 0.006 mm, smaller than 0.008 mm. The inclination angle was 1.2″, smaller than 1.5″. The Fundamental frequency was 256 Hz, larger than 120 Hz. The maximum acceleration response amplification of the sine vibration was 1.1 times. The total root mean square acceleration amplification of the random vibration was 4.2 times. The maximum dynamic stress of the sine vibration was 14.5 MPa. The maximum dynamic stress of the random vibration was 128 MPa, which of both were smaller than the yield limit of the material. The mass of the mirror subassembly was 0.72 kg, smaller than 0.8 kg.

## Declaration of Competing Interest

None.

## Acknowledgements

This research was supported by the program of The key technology that multipoint passive support of the space-based large-aperture mirror is compatible with active support (The program number is 11703027),which comes from National Natural Science Foundation of china.

## References

[1] Y.Q. Zeng, Y. Fud, J.W. Sun, et al., Summary of support structure patterns of large mirror for space remote sensor, Spacecraft Recov. Romote (2020).
[2] Jiao Shi-ju, Achievement and prospect of satellite remote sensing technology in China, Proc. SPIE (S0277-786X) 3505 (1998) 26–30.
[3] L. Fan, Research on the Lightweight Design and Support of 2m-SiC Primary Mirror for Ground-based Telescope, University of Chinese Academy of Sciences, Changchun, 2013 (in chinese).
[4] K.J. Wang, J.H. Dong, M. Xuan, et al., Compound support structure for large aperture mirror of space remote sensor, Opt. Precis. Eng. 27 (7) (2016) 1719–1730 (in chinese).
[5] P.R. Yoder, Opto-mechanical System Design, Cooperate Marcel Dekker Inc, US, 1993.
[6] J. Xue, H.B. Hu, H.Z. Song, Research on the flexible supporting structure of the optical reflector, J. Chang Chun Univ. Techonol. (Nat. Sci. Ed.) 30 (4) (2009) 457–461 (in Chinese).
[7] K.J. Wang, J.H. Dong, X.Y. Wang, et al., Back support structure design of mirror of space remote sensor, Infrared Laser Eng. 48 (7) (2019) 0718004-1-11(in chinese).
[8] F.H. Liu, Z.F. Cheng, L. Shi, et al., Design and analysis of supporting structure for rectangular mirror, Infrared Laser Eng. 44 (5) (2015) 1512–1517 (in chinese).
[9] Z.H.S. Wang, Y. Zhai, G. Mei, et al., Design of flexible support structure of reflector in space remote sensor, Opt. Precis. Eng. 18 (8) (2010) 1833–1841 .(in chinese).
[10] H.W. Xin, Y.J. Guan, J.L. Li, et al., Design of support for large aperture rectangular mirror, Opt. Precis. Eng. 19 (7) (2011) 1560–1568 (in chinese).
[11] F. Yang, G.J. Liu, Q.C. An, Error allocation of opto-mechanical system for large aperture telescope based on structure function, Opt. Precis. Eng. 23 (1) (2015) 119–221 in Chinese).
[12] Y.J. Guan, H.W. Xin, Z.L. Li, et al., Structure design and analysis of large aperture mirror subassembly, Laser Infrared 44 (7) (2014) 777–782 (in chinese).
[13] L.M. Zhang, F.G. Wang, Q.C. An, et al., Application of Bipod to supporting structure of minitype reflector, Opt. Precis. Eng. 23 (2) (2015) 438–443 (in Chinese).
[14] B. Long, T.W. Xing, S. Liao, Design of stress-relief support of aluminum mirrors and assembly assisted by SPDT, Opto-Electron. Eng. 41 (3) (2014) 1–6 (in Chinese).
[15] L. Fan, J.X. Zhang, L. Shao, et al., Axial support for large aperture primary mirror based on hydraulic whiffle-tree, Infrared Laser Eng. 42 (8) (2013) 2126–2131 (in chinese).
[16] Z.Y. Zhou, Y.G. Gao, S. Shao, et al., Design of fast steering mirror using flexible hinge, Opt. Precis. Eng. 22 (6) (2014) 1547–1554 (in chinese).
[17] C. Li, X. He, Design of lightweight of large aperture mirrors and supporting structures, Laser Technol. 39 (3) (2015) 337–340 (in chinese).
[18] Y. Gao, B. Zhang, Design and anslysis for the flexible support structure of high precision lens assembly, Opt. – Int. J. Light Electron. Opt. 175 (2018) 228–236.
[19] Q.W. Wu, H.B. Yang, J.S. Yang, et al., Design and analysis for primary mirror and its support of space camera, Opt. Tech. 30 (2) (2004) 152–156 (in Chinese).
[20] K.J. Wang, J.H. Dong, W. Li, et al., Finite element analysis of overall structure of space camera, Ome Inf. 17 (12) (2010) 81–87 (in Chinese).